Journal of Zhejiang University-SCIENCE A (Applied Physics & Engineering)
ISSN 1673-565X (Print); ISSN 1862-1775 (Online)
www.zju.edu.cn/jzus; www.springerlink.com
E-mail: jzus@zju.edu.cn

Corrosion behavior of steel rebar in coal gangue-based mortars*

Ji-xiu ZHANG†, Heng-hu SUN, Yin-ming SUN, Na ZHANG

(*Department of Materials Science and Engineering, Tsinghua University, Beijing 100084, China*)

†E-mail: zhangjixiu06@mails.tsinghua.edu.cn

Received July 22, 2009; Revision accepted Nov. 16, 2009; Crosschecked Mar. 30, 2010

Abstract: Corrosion of steel rebar is the most important durability problem of reinforced concrete. The aim of this research was to investigate the corrosion behavior of steel rebar in simulated pore solutions and gangue-blended cement mortar. The simulated pore solutions were based on the pore solution composition of gangue-blended cement. The pH and Cl^- concentration of simulated pore solutions had significant effects on corrosion potential. However, an increase in pH reduced the influence of Cl^- concentration on corrosion potential. The corrosion behavior of steel rebar in gangue-blended cement is different from that in simulated solutions. The gangue cementitious mortar surrounding steel rebar provides stable passivity environments for steel, leading to a decrease in ion diffusion coefficients. Alternating current impedance (ACI) analysis results indicated that the indicator R_c for concrete resistivity is higher for gangue mortar than for ordinary Portland cement (OPC), which improves its corrosion potential. The results from energy dispersive X-ray analysis (EDX) showed more aluminates and silicates at the rebar interface for gangue-blended cement. These aluminates improve the chloride binding capacity of hydrates in mortar, and increase the corrosion protection of steel rebar.

Key word: Steel rebar, Corrosion, Coal gangue, Electrochemical
doi:10.1631/jzus.A0900443 **Document code:** A **CLC number:** TD98

1 Introduction

Coal gangue is the solid waste from the coal industry. Gangue emissions form about 10% of coal production. The accumulated stockpile of coal gangue has reached 3.8 billion tons and it is estimated that over 200 million metric tons of this waste is impounded annually in China (National Economic and Trade Commission, 1999). The latest data from the State Bureau of Coal Mine Safety and Supervision (http://news.xinhuanet.com/fortune/2007-06/15/content_6246139.htm, accessed on July, 2007) indicate that the production capacity of additional coal mines under construction and expansion in China is estimated to more than 11 billion tons at present. Total coal production is expected to reach 31 billion tons in 2010, 5 billion tons more than the target in the "National Eleventh Five-year Plan". According to these data, emissions of this subproduct will increase to 3 billion tons annually.

At present, the comprehensive utilization rate of coal gangue is very low. The vast majority of gangue is stockpiled, not only creating local ecological and environmental problems, but also threatening the safety of the resident population. Governments and researchers have placed increasing emphasis on the comprehensive utilization of coal gangue. Studies have shown that the principal components of gangue are silicon and aluminum. It also contains a variety of clay minerals. These clay minerals yield cementitious activity during the thermal activation process (Li H.J. *et al.*, 2006; Querol *et al.*, 2008). Gangue is used in construction materials which have good prospects for comprehensive utilization. Current research is focused mainly on improving cementitious activity, and promising results have been achieved (Thompson,

* Project supported by the National Natural Science Foundation of China (No. 50674062), the National Science & Technology Pillar Program (No. 2006BAC21B03), and the Beijing Science and Technology Plan Projects (No. D07040300690000), China

1947; Li D.X. *et al.*, 2006). However, the cementitious activity is currently insufficient for these materials to qualify as suitable for use in construction (Batis and Pantazopoulou, 2005). Durability problems, especially the corrosion of reinforcement steel (Mohammed and Hamada, 2006a), limit the large-scale application of this byproduct in construction materials (Jin and Zhao, 2001; Zhang and Li, 2006). Economic losses caused by rust and corrosion are enormous (Higgins and Farrow III, 2006). In the USA, the damage caused by the corrosion process results in tremendous economic losses, amounting to around $276 billion per year (Virmani, 2002). Corrosion not only wastes a large quantity of material, but also threatens human life. Corrosion of reinforcement steel and its protection from corrosion have become urgent issues that need to be solved (Polder, 2002; Mohammed and Hamada, 2006b). Therefore, the aim of this study of steel corrosion behavior in gangue-blended cement was to provide a reference for further extensive utilization of gangue in the field of building cementitious materials.

2 Experimental

2.1 Materials

The coal gangue used in this experiment was from Fangshan, Beijing, and the clinker was from the Xingang Beijing Cement Plant. The chemical composition of the materials used in this study is shown in Table 1.

Table 1 Chemical composition of raw materials (%, w/w)

Raw material	SiO_2	Al_2O_3	CaO	K_2O	MgO	Fe_2O_3	LOI
Gangue	45.57	16.35	1.93	2.85	1.56	6.02	25.72
Clinker	21.94	5.27	64.1	1.77	1.88	2.96	0.90

LOI: loss on ignition

2.2 Experimental procedure

The gangue was broken, ground, and then calcined at 900 °C for 2 h. Deionized water was added to calcined coal gangue and ordinary Portland cement (OPC), respectively. Ion dissolution was conducted using an autoclave at 80 °C and 15 kPa. The reaction time was 6 h.

The dissolution liquid filtrate was collected. Inductively coupled plasma mass spectrometry (ICP-MS) analysis was conducted using ELAN 6000 PE (America) to test the ion and iron content (Table 2).

The simulated pore solutions of OPC and gangue were prepared according to the results shown in Table 2. OPC pore solution: 0.6 mol/L KOH+0.2 mol/L NaOH+0.01 mol/L $Ca(OH)_2$+0.01 mol Na_2CO_3. Gangue pore solution: 0.6 mol/L KOH+0.2 mol/L NaOH+0.01 mol/L $Ca(OH)_2$+0.01 mol Na_2SO_4. Cl^- was provided by sodium chloride (chemically pure). The pH value was adjusted by changing the concentration of $Ca(OH)_2$ or NaOH solutions.

Table 2 ICP results of different pore solutions (μg/ml)

Sample	Ca	Na	Si	S	Al	Sum
Gangue	243.017	67.33	10.43	305.5	2.183	628.460
OPC	365.04	211.2	5.094	2.659	—	586.176

In this investigation, the size of the sample in the simulated pore solution was 10 mm×10 mm. The surface finish was Δ6. Gangue was used to partially replace the Portland cement. The ratio of gangue to clinker to gypsum and sand was 45:50:5:250. The water to solid ratio was 0.40.

Quadrate mortar specimens of 30 mm×30 mm ×95 mm were constructed with a single rebar (7 mm diameter and 100 mm length) in the center. Specimens (per composition) were cast and then stored in a curing room at 20 °C and at a relative humidity (RH) of 95% for 24 h. The specimens were then demoulded and cured at (20±1) °C and an RH of 100% for 28 d (for all compositions).

The specimens were exposed to an aggressive treatment of 3.5% per mass NaCl solution for 24 h before the corrosion behavior test was conducted using a CHI660C electrochemical work station (China). The reference electrode was Pt and the scanning rate was 0.01 V/s. The scanning range was −2–2 V. The electrochemical response of the steel-mortar interface was recorded in the frequency interval of 10–100 kHz by means of the electrochemical impedance spectroscopy technique.

The morphology of the interface between the steel rebar and the cementitious materials was observed using a scanning electron microscope (SEM) (JSM-6460LV, JEOL, Japan) with an energy spectrum detector (Be4-U92). The rebar-mortar interface chemical composition was tested using energy dispersive X-ray analysis (EDX).

3 Results and discussion

3.1 Corrosion behavior of samples in simulated pore solutions

Fig. 1 shows the Tafel curves of steel in simulated pore solutions of different pH values. Corrosion appears to be controlled by anodic polarization. Corrosion potentials gradually increase and then stabilize as pH values increase. The increase in pH from 7 to11 leads to a positive shift in corrosion potential (Fig. 2). Although the corrosion potential continues to rise with pH, the rate reduces significantly after pH 11 is reached. No effect of pH values on corrosion current is evident. The cathode Tafel slope can be roughly divided into two pH intervals, 7–10 and 11–14. Little change in slope can be seen within each interval, but the slope decreases significantly from the 7–10 to the 11–14 interval. At the same time, the anodic Tafel slope of the curve increases (Table 3). This indicates that the corrosion is controlled by the anodic polarization process. The surface of the steel rebar changes with pH value. The passive film on the surface of rebar in simulated pore solutions of higher pH values hinders the electron mobility between the anode and the solution. Thus, the effect of anodic control of the whole process is more obvious.

The polarization curves of steel rebar in NaCl solutions with concentrations of 0.2%, 0.6%, 1.0%, 1.4%, 1.8%, or 2.0% are shown in Fig. 3. The corresponding parameters are shown in Table 4. Fig. 4 shows the curve of corrosion potential against Cl^- concentration. This curve can be divided into 4 intervals: 0.1%–0.2%; 0.4%–0.8%; 0.8%–1.4% and 1.4%–2.0%. In the intervals of 0.1%–0.2% and 0.8%–1.4%, the corrosion potentials decrease rapidly compared with those in the other two intervals. The

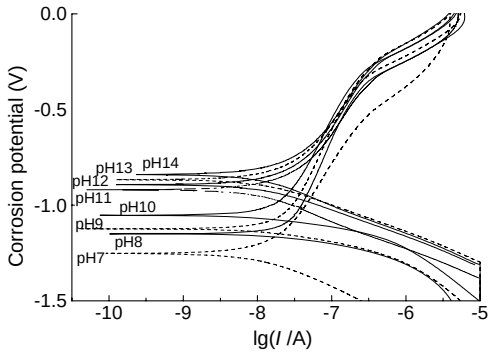

Fig. 1 Tafel curves of samples in simulated pore solutions of different pH valves. *I* is the current, A

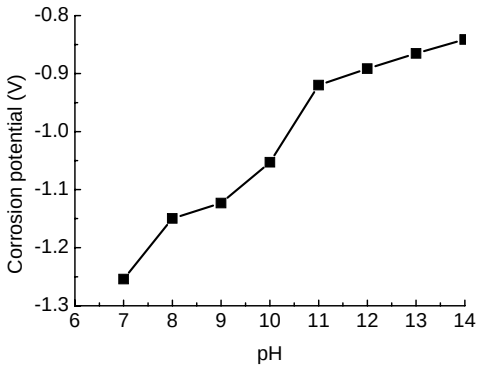

Fig. 2 Corrosion potential curve of a steel rebar at different pH values

Table 3 Results for Tafel curves in solutions of different pH values

pH	Current (A)	Cathodic Tafel slope (1/V)	Anodic Tafel slope (1/V)	Polarization resistance (Ω)
7	1.219E−8	7.386	1.564	3985263.0
8	3.007E−8	10.266	1.703	1208077.5
9	1.815E−8	11.230	1.705	1852167.0
10	1.612E−8	11.426	1.800	2039505.6
11	1.526E−8	6.676	1.988	3288703.5
12	9.692E−9	5.493	2.145	5872631.0
13	1.558E−8	8.008	1.854	2829146.5
14	1.661E−8	6.657	1.906	3056154.0

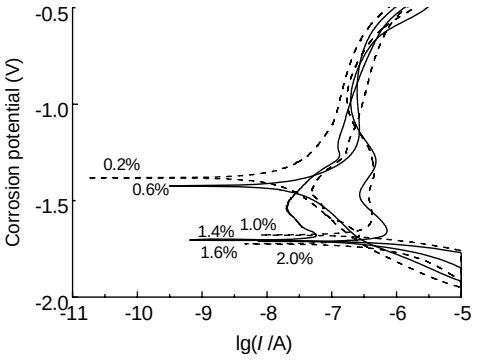

Fig. 3 Tafel curves of steel rebar in solutions of different Cl^- concentrations (values in the plot). *I* is the current, A

Table 4 Results for Tafel curves for solutions with different Cl^- concentrations

Cl^- concentration	Current (A)	Cathodic Tafel slope (1/V)	Anodic Tafel slope (1/V)	Polarization resistance (Ω)
0.2	2.858E−8	5.018	1.473	2343620.0
0.6	6.003E−8	4.733	1.087	1244483.6
1.0	2.814E−8	7.227	1.205	1832498.4
1.4	2.635E−7	9.990	1.347	145539.1
1.8	6.426E−7	7.492	1.152	78273.7
2.0	2.305E−5	0	0.817	23088.8

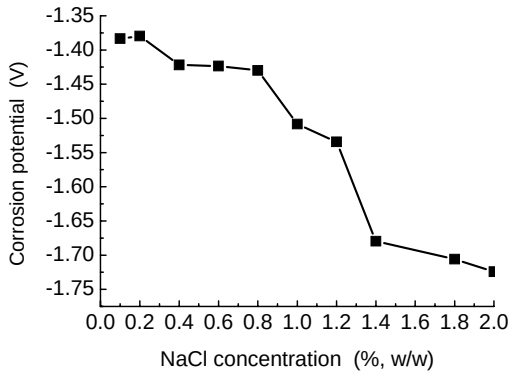

Fig. 4 Correlation between corrosion potential and Cl^- concentration

increase in Cl^- concentration improves the corrosion current of steel rebar, especially in solutions with Cl^- concentrations of 1.4% or 2.0%.

The acceleration of the corrosion process by chloride ions has been recognized previously (Sujjavanich, 2005; Fajardo *et al.*, 2009). However, corrosion does not start until the Cl^- concentration reaches or exceeds a certain threshold (Radhakrishna *et al.*, 2005). This limiting value of Cl^- concentration is called the chloride threshold level (CTL) or critical chloride content (CCC). This indicator is very important and has been studied by many researchers (Hussain and AlGahtani, 1996; Morris *et al.*, 2004). Many factors have been identified that temperature, water-solid ratio, cement type, porosity, and the pH value of the pore solution can affect the CTL. Because of interactions between factors (Rasheeduzzafar, 1992) and the use of different testing methods, great variation has been found among estimates of the CTL. Electrochemical technology is the method most commonly used to study the CTL. The CTL can be found by examining changes in corrosion potential. In this experiment the corrosion potentials and corrosion currents both changed with the chloride ion concentration. But the corrosion potential was more sensitive than the corrosion current to the Cl^- concentration. Therefore, according to the changes in corrosion potential, the observed CTL was 0.4%–0.8%. This result is very close to Henriksen's 0.3%–0.7% (Hussain *et al.*, 1995).

The mechanism of the depassivation of steel rebar by Cl^- is still not clear, but many scholars believe that the capacities of Cl^- and OH^- to combine with Fe^{2+} determine whether the process is passivate or depassivate. If the concentration of OH^- is greater than that of Cl^- the steel surface will be passivated, otherwise it will be depassivated. Therefore, the relationship between the pH value and Cl^- concentration plays a very important role in steel rebar corrosion (Berkely and Pathmanaban, 1990). The curves of corrosion potential against Cl^- concentration of steel rebar in solutions of different pH values are shown in Fig. 5.

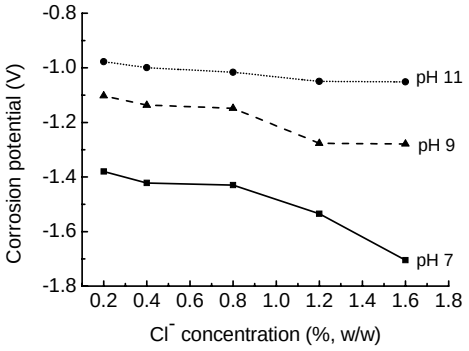

Fig. 5 Curves of corrosion potential against Cl^- concentration of steel rebar in solutions of different pH

An increase in the Cl^- concentration of the solution (pH 7) caused a significant negative shift in the corrosion potential. The effect of Cl^- concentration on corrosion potential weakened as pH increased. There was a clear change in corrosion potential with increasing Cl^- concentration until pH 11 was reached.

Hausmann (1967) showed that steel rebar could be protected in solutions of pH above 11.6 and C_{Cl^-}/C_{OH^-} below 0.6. But our results showed that a pH value above 11 weakened the effects of Cl^- concentration on corrosion potential. A high alkali environment around the steel rebar may be more important than the ratio of Cl^- to OH^- concentrations.

3.2 Corrosion behavior of steel rebar in mortar

The corrosion behavior of steel rebar in OPC and gangue-blended cement is shown in Fig. 6. Results for Tafel curves in mortar are shown in Table 5. The corrosion potentials of steel rebar in OPC shift negatively to a lower potential range (Fig. 6). A clear potential negative shift of about 0.189 V was observed. The linear polarization resistance was higher than that found in gangue mortar. This leads the corrosion current density being lower in OPC mortar. The corrosion potential of steel rebar shifted positively in gangue cementitious mortar. However, the corrosion current density increased slightly at the same time. To

discern the mechanism behind the observed difference in corrosion potential and corrosion current density, the AC impedance (ACI) technique was used.

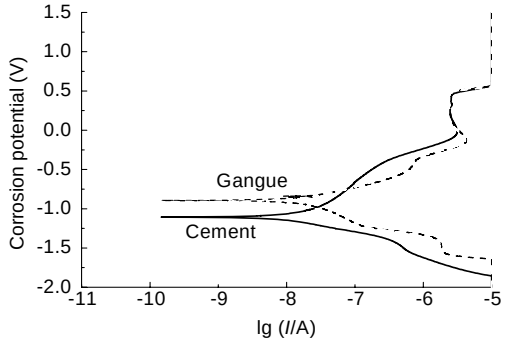

Fig. 6 Tafel curves of steel rebar in mortar. *I* is the current, A

Table 5 Results for Tafel curves in mortar

Sample	Current (A)	Cathodic Tafel slope (1/V)	Anodic Tafel slope (1/V)	Polarization resistance (Ω)
Cement	1.366E−8	6.157	1.583	4112264.8
Gangue	2.678E−8	4.360	1.214	2913202.5

ACI spectra of steel rebar in mortar are shown in Fig. 7. A frequency of 10–1×10^5 Hz was selected for this measurement. The corresponding equivalent circuit is depicted in Fig. 8, where R_c is the concrete resistivity, and R_f is the resistance of rebar passive film in alkaline pore solution. C_f is the capacitance of passive film and R_p is the charge transfer resistance of corrosion (i.e., the polarization resistance in DC measurement). C_d is the double layer capacitance and Z_d is the diffusion impedance of an active ion in the oxidation and reduction process (i.e., the Warburg impedance).

In the ACI diagram, the arc disappears at high-frequency in contrast to a typical ACI diagram of concrete (Shi *et al.*, 2000), showing that the electrochemical polarization control is very weak. This corrosion process is diffusion-controlled. The results of equivalent circuit analysis show that the concrete resistivity R_c of gangue-blended cement is more than that of OPC (Table 6). The concrete resistivity R_c

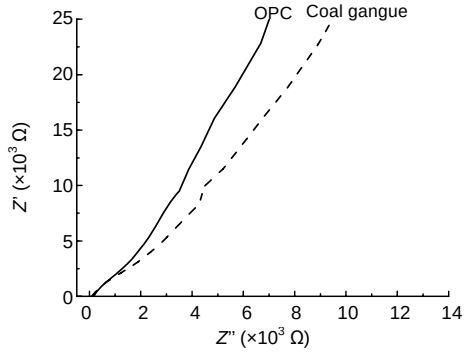

Fig. 7 ACI diagram of steel rebar in mortar

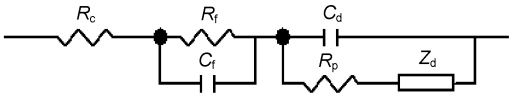

Fig. 8 Equivalent circuits of steel rebar corrosion in mortar

is determined by the type of concrete. Generally, concrete with higher R_c has stronger rebar anti-corrosion ability. R_f is the resistance of rebar passive film in alkaline pore solution. $R_f=\chi_f\rho_f$, where χ_f is the film thickness and ρ_f is the passive film resistivity which is determined by the concrete species (Shi and Chen, 1998; Xu, 1994). In our experiment, the passive film resistance, R_f, of gangue-blended cement was similar to that of OPC. This indicated that although the blended gangue decreases the relative content of calcium hydroxide, there is little change in the passive film. The charge transfer resistance of corrosion R_p and Warburg impedance Z_d of gangue-added cement are lower than those of OPC. This is because of the porosity difference of the mortar. Gangue contains clay minerals whose crystalline phase decomposes and yields active silica or alumina when calcined or spontaneously combusted. These active silica or alumina have a strong adsorption ability which reduces the fluidity of a gangue cement system at the same water-cement ratio. Pore structure was studied using a mercury injection porosimetry technique. The porosity and average pore size of gangue cement mortar are 28.41% and 29.4 nm, respectively, which are higher than those of OPC (19.22% and 16.3 nm,

Table 6 Analysis results of equivalent circuits

Sample	R_c	R_f	C_f	C_d	R_p	Z_d	Error
Gangue	147.20	3.25E+04	9.08E−05	2.50E−05	6.03E−07	7.67E−06	0.0862
OPC	134.77	3.40E+04	1.26E−05	2.16E−05	5.00E−05	1.21E−05	0.0875

respectively). The difference in pore structure is also the reason why the corrosion current increases in the gangue-blended reinforcement system.

3.3 Interface of steel rebar and mortar

The morphologies of interfaces of steel rebar in OPC and gangue cementitious material mortar are shown in Fig. 9. SEM photos show many different regions on the interface. The boundaries of these regions in OPC are more clearly defined than those in gangue cementitious material. EDX has been used to study chemical composition in these regions (Fig. 9b).

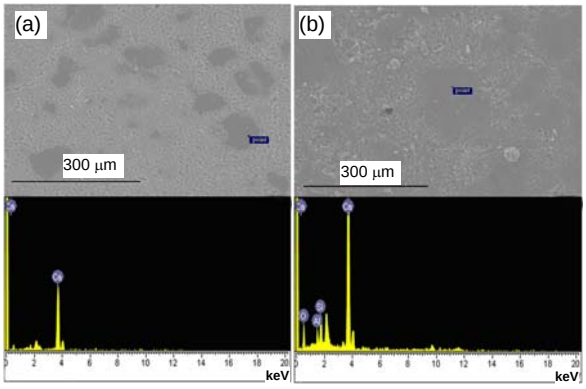

Fig. 9 Interfaces of steel rebar in (a) OPC and (b) gangue cementitious mortar

The principal chemical component of OPC is Ca. However, Si and Al elements were also found in these regions in gangue-blended cement. Many studies have shown that Cl^- can combine with C_3A to produce $3CaO{\cdot}Al_2O_3{\cdot}CaCl_2{\cdot}10H_2O$ which is known as F salt (Townsend *et al.*, 1981; Chen and Mahadevan, 2008). Many scholars suggested that the content of C_3A could be used to measure the consolidation capability of chloride ions in cementitious material. EDX results showed that the phase of the rebar-OPC interface was calcium hydroxide. Calcium hydroxide could provide a high alkaline solution around a steel rebar to retain steel rebar passivity but it is unstable and will be consumed by carbonation. However, the Cl^- can not be consolidated in the system without aluminates even in high concentrations of calcium hydroxide. Free Cl^- greatly accelerates corrosion in steel rebar, but in gangue-blended cement there is not only calcium hydroxide to maintain a high alkali environment, but also aluminates to consolidate Cl^-. These phases provide dual protection for steel rebar.

4 Conclusion

1. An increase in pH ranging from 7–11 greatly improves the corrosion potential of reinforcement steel. Although the corrosion potential continues to increase when the pH rises above 11, the rate of increase is significantly reduced.

2. The corrosion potential curve in solutions with different Cl^- concentrations could be divided into four intervals: 0.1%–0.2%; 0.4%–0.8%; 0.8%–1.4% and 1.4%–2.0%. From 0.1%–0.2% and from 0.8%–1.4%, the corrosion potentials decreased significantly. But in the other two intervals there was a slower rate of decline. The corrosion current of steel rebar increased with increasing Cl^- concentration, especially in solutions of 1.4% and 2.0% Cl^- concentration.

3. The increase in Cl^- concentration in a solution of pH 7 caused a negative shift in the corrosion potential. The effect of Cl^- concentration on corrosion potential weakened with increasing pH, especially above pH 11.

4. The corrosion potential of steel rebar in coal gangue cementitious material is higher than that in OPC because of a difference in R_c.

5. There are many different regions, like islands, at the interface. The morphology of these regions differs. More Si and Al elements were observed in these island regions in gangue cementitious material than in OPC. The aluminate phases improve Cl^- consolidation and steel rebar anti-corrosion performance.

References

Batis, G., Pantazopoulou, P., 2005. The effect of metakaolin on the corrosion behavior of cement mortars. *Cement & Concrete Composites*, **27**(1):125-130. [doi:10.1016/j.cemconcomp.2004.02.041]

Berkely, K.G.C., Pathmanaban, S., 1990. Cathodic Protection of Reinforcement Steel in Concrete. Butterworths & Co. Ltd., London.

Chen, D., Mahadevan, S., 2008. Chloride-induced reinforcement corrosion and concrete cracking simulation. *Cement & Concrete Composites*, **30**(3):227-238.

Fajardo, G., Valdez, P., Pacheco, J., 2009. Corrosion of steel rebar embedded in natural pozzolan based mortars exposed to chlorides. *Construction and Building Materials*, **23**(2):768-774. [doi:10.1016/j.conbuildmat.2008.02.023]

Hausmann, D.A., 1967. Steel corrosion in concrete: how does it occur. *Materials Protection*, **6**(11):19-23.

Higgins, C., Farrow III, W.C., 2006. Tests of reinforced concrete beams with corrosion damaged stirrups. *ACI*

Structural Journal, **1**:133-141.

Hussain, S.E., Rasheeduzzafar, S., Al-Musallam, A. Al-Gahtani, A.S., 1995. Factors affecting threshold chloride for reinforcement corrosion in concrete. *Cement and Concrete Research*, **25**(7):1543-1555.

Hussain, S.E., AlGahtani, A.S., 1996. Chloride threshold for corrosion of reinforcement in concrete. *ACI Materials Journal*, **94**(6):534-538.

Jin, W.L., Zhao, Y.X., 2001. Effect of corrosion on bond behavior and bending strength of reinforcement concrete beams. *Journal of Zhejiang University-SCIENCE*, **2**(3):298-308.

Li, D.X., Song, X.Y., Gong, X.X., 2006. Research on cementitious behavior and mechanism of pozzolanic cement with coal gangue. *Cement and Concrete Research*, **36**(9):1752-1759. [doi:10.1016/j.cemconres.2004.11.004]

Li, H.J., Sun, H.H., Xiao, X.J., 2006. Mechanical properties of gangue-containing aluminosilicate based cementitious materials. *Journal of University of Science and Technology Beijing*, **13**(2):183-189.

Mohammed, T.U., Hamada, H., 2006a. Corrosion of horizontal bars in concrete and method to delay early corrosion. *ACI Materials Journal*, **103**(5):303-311.

Mohammed, T.U., Hamada, H., 2006b. Corrosion of steel bars in concrete with various steel surface conditions. *ACI Materials Journal*, **103(**4):233-242.

Morris, W., Vico, A., Vázquez, M., 2004. Chloride induced corrosion of reinforcing steel evaluated by concrete resistivity measurements. *Electrochimica Acta*, **49**(25):4447-4453. [doi:10.1016/j.electacta.2004.05.001]

National Economic and Trade Commission, 1999. Technology Policy Points of Gangue Comprehensive Utilization Technology Policy Points. Chinese Ministry of Science and Technology.

Polder, R.B., 2002. Characterization of chloride transport and reinforcement corrosion in concrete under cyclic wetting and drying by electrical resistivity. *Cement & Concrete Composites*, **24(5)**:427-435. [doi:10.1016/S0958-9465(01)00074-9]

Querol, X., Izquierdo, M., Monfort, E., 2008. Environmental characterization of burnt coal gangue banks at Yangquan, Shanxi Province, China. *International Journal of Coal Geology*, **75**(2):93-104. [doi:10.1016/j.coal.2008.04.003]

Rasheeduzzafar, 1992. Influence of cement composition on concrete durability. *ACI Materials Journal*, **89**(6):574-586.

Radhakrishna, G., Pillai, D., Trejo, 2005. Surface condition effects on critical chloride threshold of steel reinforcement. *ACI Materials Journal*, **102**(2):103-109.

Shi, M.L., Chen, Z.Y., 1998. Study of AC impedance on the porous structure of hardened cement paste. *Journal of Building Materials*, **1**(1):30-35.

Shi, M.L., Chen, Z.Y., Sun, J., Hu, Y., 2000. Electrochemical research on the hydration process of Cement(II)—ACIS of hardened cement paste under DC polarization. *Journal of Building Materials*, **3**(3):218-222.

Sujjavanich, S., Sida, V., 2005. Chloride permeability and corrosion risk of high-volume fly ash concrete with mid-range water reducer. *ACI Materials Journal*, **102**(3):177-182.

Thompson, J.B., 1947. Role of aluminum in the rock-making silicates. *Bulletin of the Geological Society of America*, **58**:12-32.

Townsend, H.E., Cleary, H.J., Allegra, L., 1981. Breakdown of oxide films in steel exposure to chloride solutions. *NACE Corrosion*, **37**:384-391.

Virmani, Y.P., 2002. Corrosion Costs and Preventive Strategies in the United States. Federal Highway Administration Report No. FHWA-RD-01-156.

Xu, Z.Z., 1994. Development in electrochemistry of cement and concrete science—AC impedance spectroscopy theory. *Journal of the Chinese Ceramic Society*, **22**(2):173-180.

Zhang, Y.L., Li, Q.L., 2006. Electrochemical study on semiconductive properties of the passive film on rebar in concrete. *Journal of Zhejiang University-SCIENCE A*, **7**(8):1447-1452. [doi:10.1631/jzus.2006.A1447]